THE BELL SYSTEM TECHNICAL JOURNAL
Vol. 55, No. 7, September 1976
Printed in U.S.A.

Transmission vs Transverse Offset for Parabolic-Profile Fiber Splices With Unequal Core Diameters

By C. M. MILLER

(Manuscript received March 16, 1976)

A geometrical optics model is presented that is based on defining a local numerical aperture as a function of fiber radius with a uniform power distribution. Transmission vs transverse offset characteristics for parabolic-profile fiber splices are calculated for unequal fiber-core diameters. We show that the often-used assumptions of equal-mode excitation, equal-mode attenuation, and no-mode coupling are not adequate to calculate realistic transmission vs offset characteristics. Splice-loss measurements with long fiber lengths on each side of the splice show less than the calculated sensitivity to small offsets and greater than the calculated sensitivity to large offsets.

I. INTRODUCTION

Accurate transverse alignment is difficult to obtain in fiber optic splices primarily due to the small size of optical fibers. Many splicing techniques[1,2,3] use grooves or channels and are dependent on fiber outer diameter (OD) for transverse alignment. Experience thus far indicates that OD variations as small as ± 1 percent can be achieved on a single long fiber; however, fiber-to-fiber variations for fibers drawn at different times may be considerably greater. Small fluctuations in core-diameter-to-OD ratios are also expected. When the receiving fiber core is smaller than the transmitting fiber core, a loss occurs even with perfect transverse axial alignment.

Thiel[4] and Henderson[5] have reported transmission vs offset for equal-core-diameter, step-profile fiber splices and Pugh[6] has considered core-diameter ratios less than one (receiving fiber smaller than transmitting fiber) for step-profile fiber splices. Calculated values for transmission vs offset for equal-core-diameter, parabolic-profile fiber splices have been obtained earlier by the author.[7]

Transmission vs offset for parabolic-profile fiber splices with unequal core diameters is calculated in this paper. In addition, transmission vs offset-measurement data for equal-core-diameter, parabolic-profile fiber splices are presented. We found that the theoretical model gives pessimistic results for the equal-diameter case for the region of primary interest (offsets less than 0.8 core radius). Measured transmission is less than the model for offsets greater than 0.8 core radius.

II. ASSUMPTIONS

The solid angle defined by the local numerical aperture (NA) of the fiber at every point on the core is assumed to contain a uniform power distribution. This assumption is consistent with equal-mode excitation, equal-mode attenuation, and no-mode coupling.[8] Consider the profile

$$\eta(r) = \eta_0 \left[1 - 2\Delta \left(\frac{r}{R}\right)^{\alpha}\right]^{\frac{1}{2}} \quad \text{for} \quad r < R, \tag{1}$$

where

$\Delta = (\eta_0 - \eta_c)/\eta_0$ is small.
η_0 = refractive index at center of core.
η_c = refractive index of cladding.
α = a parameter between 1 and ∞.
R = fiber core radius.

The NA as a function of radius is then

$$\text{NA}(r) = [\eta(r)^2 - \eta_c^2]^{\frac{1}{2}}, \tag{2}$$

or

$$\text{NA}(r) \cong \eta_0\sqrt{2\Delta}\left[1 - \left(\frac{r}{R}\right)^{\alpha}\right]^{\frac{1}{2}}. \tag{3}$$

Since uniform power per unit solid angle is assumed transmitted for each incremental area of the core within the angle

$$\phi(r) = \sin^{-1}[\text{NA}(r)/\eta(r)], \tag{4}$$

the total power, P_T, equals

$$P_T \cong P(0) \int_0^{2\pi} \int_0^{R} \left[1 - \left(\frac{r}{R}\right)^{\alpha}\right] r dr d\theta, \tag{5}$$

or

$$P_T = \pi R^2 \alpha P(0)/(\alpha + 2), \tag{6}$$

where $P(0)$ is a constant dependent on the input power Δ and η_0.

When the fiber cores are offset, the total power received at a given point is assumed to be limited by the transmitting or receiving NA, whichever is the minimum at that point.

III. GENERAL APPROACH FOR THE PARABOLIC PROFILE ($\alpha = 2$)

For the case of equal fiber-core diameters, the locus of equal NA is a straight line, as shown in Fig. 1. The NA function is integrated over the area of overlap bounded by a circle and a straight line. The resulting integral for received power in region I, where the transmitting fiber has the minimum NA, is

$$P_R = 2P(0) \int_0^{\cos^{-1}(d/2R_T)} \int_{d/2\cos\theta}^{R_T} \left[1 - \left(\frac{r}{R_T}\right)^2\right] r dr d\theta. \tag{7}$$

For region II, where the receiving fiber NA function has the minimum NA, a positive translation of the NA function must be made. The receiving NA function, translated an amount d and referenced to the center of the transmitting fiber, equals

$$\text{NA}(r) \cong n_0 \sqrt{2\Delta} \left[1 - \left(\frac{r^2 - 2dr\cos\theta + d^2}{R_R^2}\right)\right]. \tag{8}$$

Four separate cases are considered to calculate transmission vs offset for unequal core diameters. If K is the ratio of the radius of the receiving fiber to the radius of the transmitting fiber, $K = R_R/R_T$, and d = offset, then the four cases are as follows:

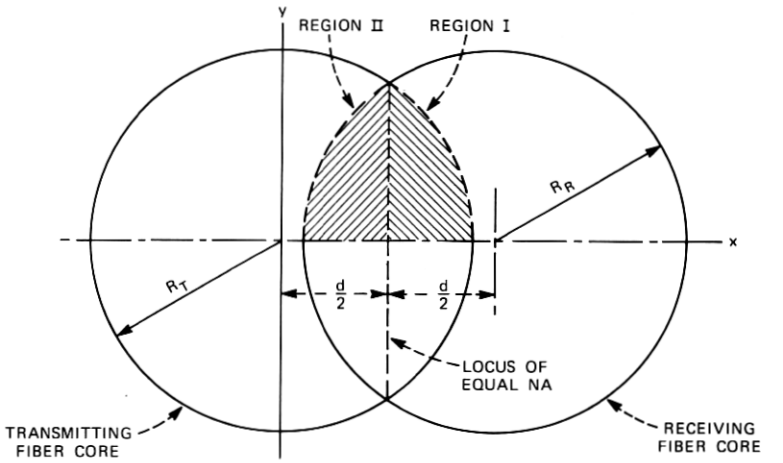

Fig. 1—Regions of overlap for offset fiber cores ($R_T = R_R$).

Case I

See Fig. 2. $d/R_T < K - 1$ for $K > 1$. Core boundaries do not intersect and $R_R > R_T$.

Case II

See Fig. 3. $d/R_T > K - 1$ for $K > 1$. Core boundaries intersect and $R_R > R_T$.

Case III

See Fig. 4. $d/R_T < 1 - K$ for $K < 1$. Core boundaries do not intersect and $R_T > R_R$.

Case IV

See Fig. 5. $d/R_T > 1 - K$ for $K < 1$. Core boundaries intersect and $R_T > R_R$.

For Cases I and III, areas of overlap are circles and the integrals are easily written and solved for the transmission. The resulting equations are shown on Figs. 2 and 4. For Cases II and IV, some areas of overlap are bounded by arcs of circles, and integrals for these areas are tedious to solve. The approach used for these cases is to divide

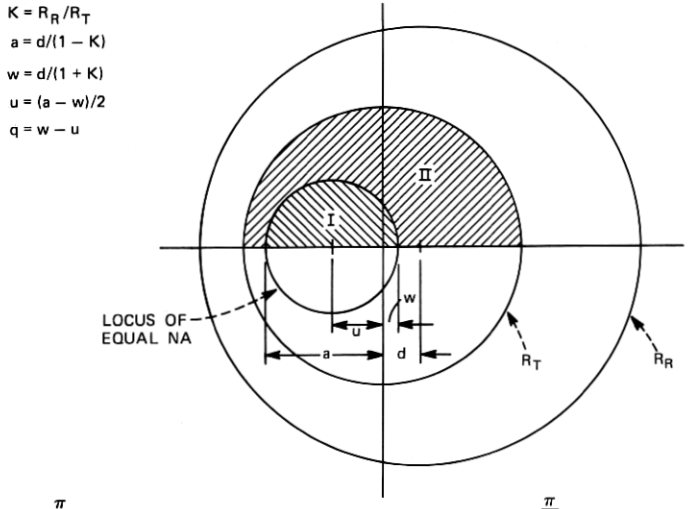

$$P_I = 2\int_0^{\frac{\pi}{2}}\int_0^{q}\left[1-\left(\frac{r}{R_R}\right)^2+\frac{2(d-u)r\cos\theta}{R_R^2}-\frac{(d-u)^2}{R_R^2}\right]r\,dr\,d\theta\,;\quad P_{II}=\frac{P_{TOT}}{2}-\int_0^{\frac{\pi}{2}}\int_0^{q}2\left[1-\left(\frac{r}{R_T}\right)^2-\frac{2ur\cos\theta}{R_T^2}-\frac{u^2}{R_T^2}\right]r\,dr\,d\theta$$

$$T=\frac{2(P_I+P_{II})}{P_{TOT}}=1+\frac{4q^2}{R_T^2}\left[\left(1-\frac{1}{K^2}\right)\left(\frac{q^2}{2}+\frac{4qu}{3\pi}+\frac{u^2}{2}\right)+\frac{d}{K^2}\left(\frac{4q}{3\pi}+u-\frac{d}{2}\right)\right]$$

Fig. 2—$d < R_R - R_T$.

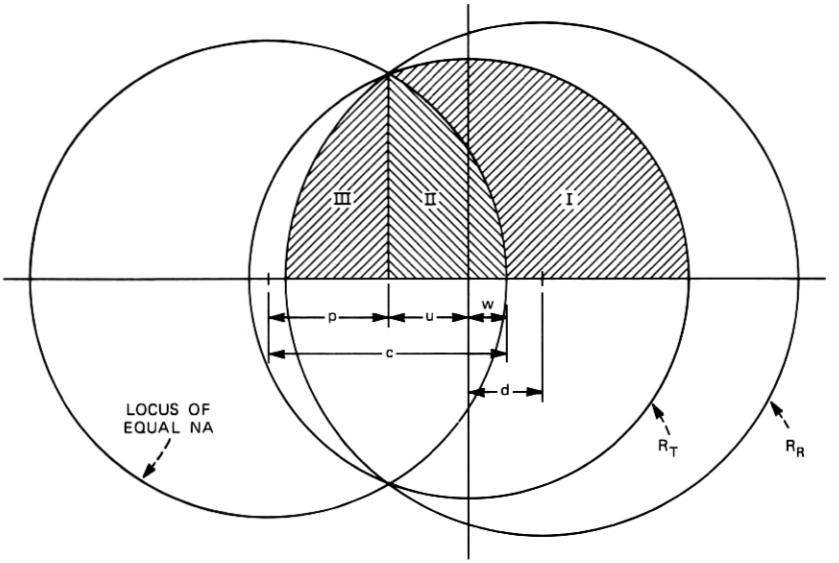

Fig. 3—$d > R_R - R_T$.

the areas of overlap into sections which are bounded by a circle and a straight line and to combine these sections to obtain the required geometry. All integrals then have the form suggested by eqs. (7) and (8) and can be segmented into the following three integral forms.

$$\int_0^{\cos^{-1}(a/b)} \int_{a/\cos\theta}^{b} r dr d\theta = \frac{b^2}{2} \cos^{-1}\frac{a}{b} - \frac{a}{2}\sqrt{b^2 - a^2}. \tag{9}$$

$$\int_0^{\cos^{-1}(a/b)} \int_{a/\cos\theta}^{b} r^2 \cos\theta \, dr d\theta = \tfrac{1}{3}\sqrt{(b^2 - a^2)^3}. \tag{10}$$

$$\int_0^{\cos^{-1}(a/b)} \int_{a/\cos\theta}^{b} r^3 \, dr d\theta = \frac{b^4}{b} \cos^{-1}\frac{a}{b} - \frac{a}{12}\sqrt{(b^2 - a^2)^3} - \frac{a^3}{4}\sqrt{b^2 - a^2}. \tag{11}$$

These integrals were computer-programmed and summed to calculate transmission vs offset. Closed form expressions were not obtained due to the large number of terms involved. The combination of integrals for cases II and IV is given in the Appendix.

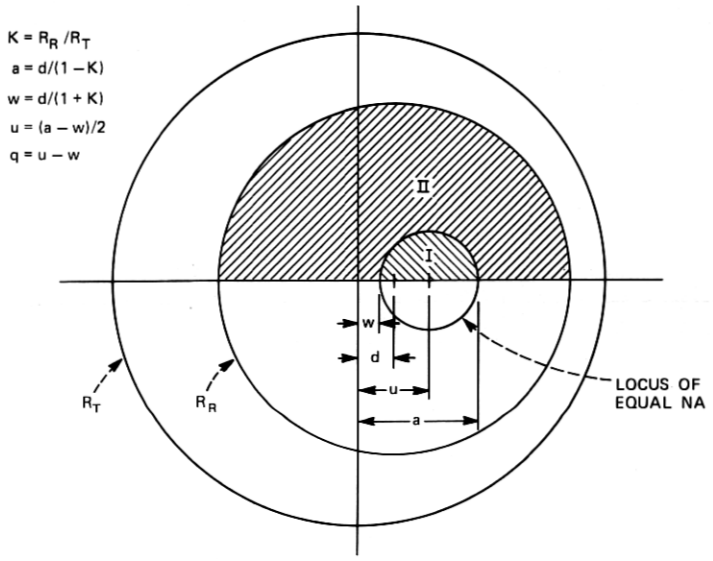

$$P_I = 2\int_0^{\frac{\pi}{2}}\int_0^{q}\left[1-\left(\frac{r}{R_T}\right)^2+\frac{2ur\cos\theta}{R_T^2}-\frac{u^2}{R_T^2}\right]r\,dr\,d\theta \;;\; P_{II} = 2\int_0^{\frac{\pi}{2}}\int_0^{q}\left[1-\left(\frac{r}{R_R}\right)^2\right]r\,dr\,d\theta - 2\int_0^{\frac{\pi}{2}}\int_0^{q}\left[1-\left(\frac{r}{R_R}\right)^2\right.$$
$$\left.+\frac{2(u-d)r\cos\theta}{R_R^2}-\frac{(u-d)^2}{R_R^2}\right]r\,dr\,d\theta$$

$$T = K^2 + \frac{4q^2}{R_T^2}\left[\left(\frac{1}{K^2}-1\right)\left(\frac{q^2}{2}-\frac{4qu}{3\pi}+\frac{u^2}{2}\right)+\frac{d}{K^2}\left(\frac{4q}{3\pi}-u+\frac{d}{2}\right)\right]$$

Fig. 4—$d < R_T - R_R$.

IV. RESULTS OF CALCULATIONS

Figure 6 is the resulting plot of transmission (percent) vs offset (transmitting fiber-core radius) for $K = 1.05$, 1.00, and 0.95. Also shown are results calculated for the step profile for $K = 1.00$ and 0.95. These calculations show a 33-percent greater sensitivity to offset for the parabolic profile and approximately the same sensitivity to K as the step profile. Figure 7 is a family of curves for small offsets. For zero offset, the transmission equals 1 for $K > 1$ and equals K^2 for $K < 1$, as in the step profile. For offsets less than $R_T - R_R$ for $K < 1$, the parabolic profile exhibits a dependence on offset, whereas the step profile is constant. The reduction in transmission due to this effect is only 0.7 percent at 0.05 core-radius offset for $K = 0.95$. The slope discontinuities in the parabolic case in Fig. 7 result from the 0.01 core-radius offset increment selected. Curves for transmission vs offset are smooth except at the point $d = R_T - R_R$, where a discontinuity in the slope may exist.

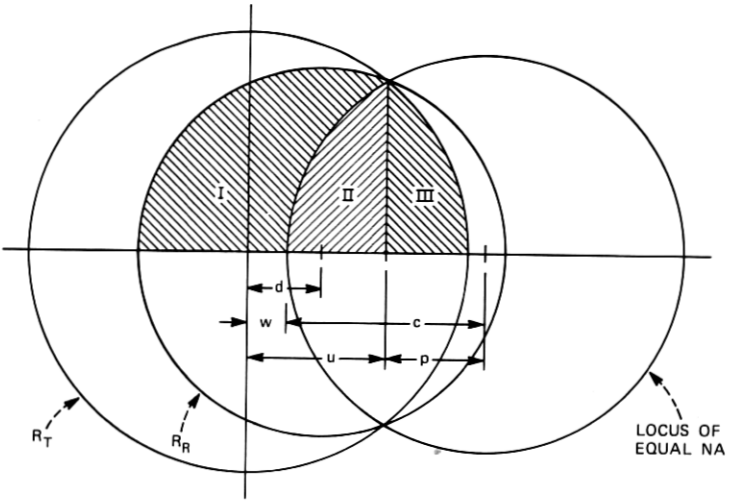

$$k = R_R / R_T$$

$$u = (1/2d)\,(R_T^2 - R_R^2 + d^2)$$

$$w = d/(1 + K)$$

$$c = \frac{-2uw + w^2 + R_T^2}{2(u - w)}$$

$$p = c + w - u$$

Fig. 5—$d > R_T - R_R$.

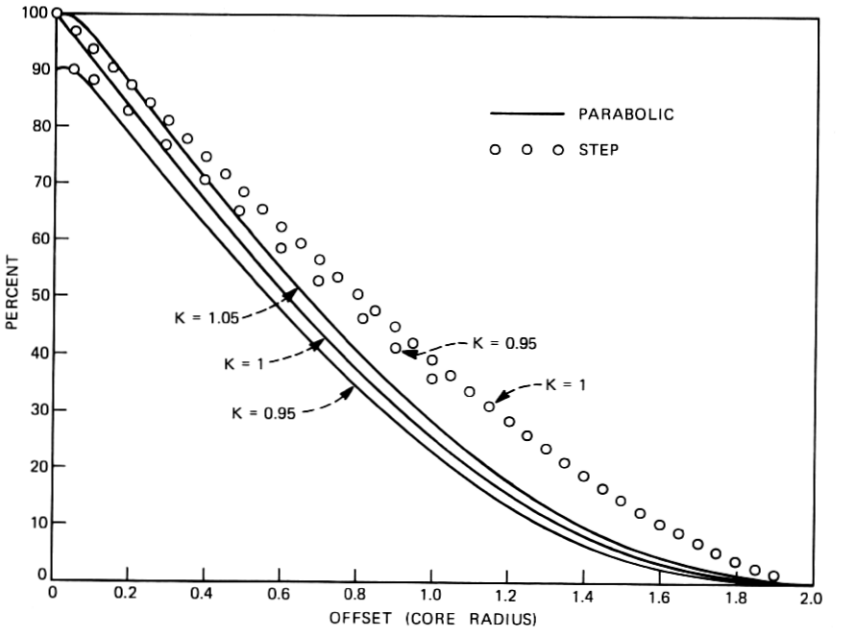

Fig. 6—Calculated transmission vs transverse offset.

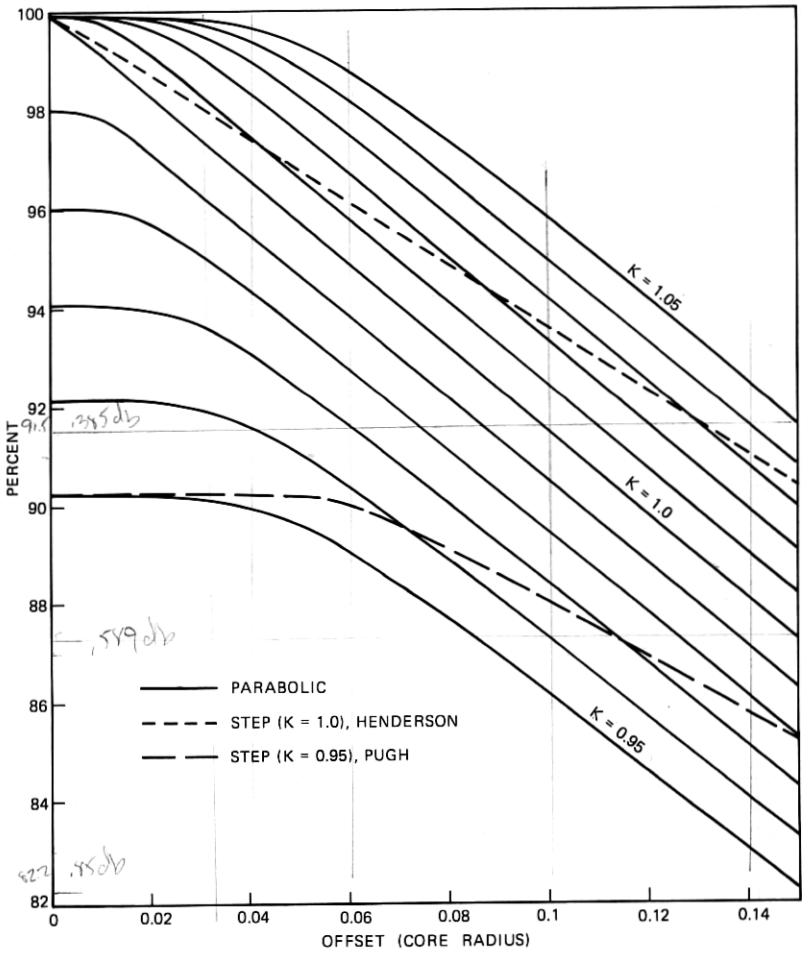

Fig. 7—Calculated transmission vs transverse offset for small offsets.

V. COMPARISON OF CALCULATIONS AND MEASUREMENTS

Several investigators have seen indications[9,10] that the sensitivity to small offsets is significantly less than the calculated values for parabolic fiber splices. These measurements[9,10] were made with short fibers on each side of the splice and the launched mode distribution probably differed greatly from the uniform power distribution assumed here.

A measurement of transmission vs offset was made with 500 meters of Corning fiber on each side of the splice subsequent to measuring the 100-percent transmission level. A helium-neon laser with an expanded beam and a 20X objective lens were used to completely fill the fiber NA. Two tabs were placed near the center of the 1-km parabolic CGW

fiber, about 4 inches apart, and the fiber was scored and broken between these tabs. A single break was made and the same ends were realigned on a microscope slide against a thin straightedge with the tabs used to obtain rotational alignment. Glycerin was used as the index-matching material and a cover slip held the ends in position under a microscope. The 100-percent level was again obtained and transverse offset was introduced in the splice and photographed.

Figure 8 shows the result of the transmission vs offset measurement. The sensitivity to offset for small offsets was less than predicted by theory, and greater than predicted for large offsets. The crossover point is approximately 0.8 core radius. For small offsets the reduction in sensitivity to offset is approximately the same as one would expect for a 10-percent oversized receiving fiber ($K = 1.1$).

The use of the geometrical optics approximation has been corroborated by comparison with the wave analysis of Marcuse.[12] The conclusion is that the assumption of equal-mode excitation, equal-mode attenuation, and no-mode coupling is not adequate to calculate splice transmission sensitivity to offset. The calculated transmission with core-diameter mismatch shows trends that can be used to obtain relative effects only. The long fiber length measurements of transmission vs offset can be used as design data for setting required alignment tolerances.

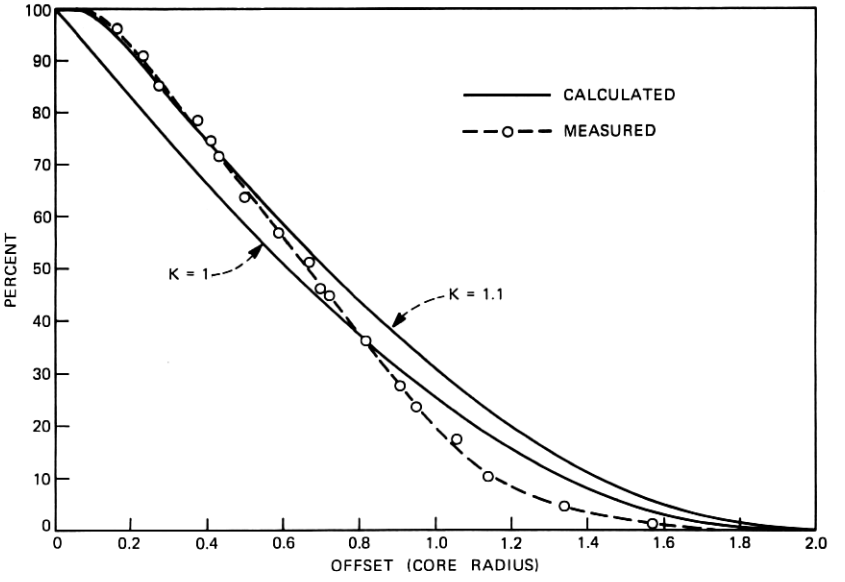

Fig. 8—Comparison of calculated and measured transmission vs transverse offset.

Current work by Gloge[13] indicates that the assumption of a sharp cutoff of power at the boundary of the solid angle defined by local NA could cause the discrepancies noted here. The model used in this paper is extended by Gloge to include a nonuniform power distribution across the solid angle defined by the local NA.

VI. ACKNOWLEDGMENT

The author is grateful to A. W. Miller for his help with the computer programs and plots.

APPENDIX

Integrals for Cases II and IV

A.1 Case II (Fig. 3) $d/R_T > 1 - K$ for $K > 1$.

$$P_{\mathrm{I}} = P_{\mathrm{tot}} - 2\int_0^{\cos^{-1}(-u/RT)} \int_{-u/\cos\theta}^{RT} \left[1 - \left(\frac{r}{R_T}\right)^2\right] r\,dr\,d\theta - 2\int_0^{\cos^{-1}(p/c)} \int_{p/\cos\theta}^{c} \left[1 - \frac{r^2}{R_T^2} - \frac{2r(c-w)\cos\theta}{R_T^2} - \frac{(c-w)^2}{R_T^2}\right] r\,dr\,d\theta$$

$$P_{\mathrm{II}} = 2\int_0^{\cos^{-1}(p/c)} \int_{p/\cos\theta}^{c} \left[1 - \frac{r^2}{R_R^2} - \frac{2r(c+d-w)\cos\theta}{R_R^2} - \frac{(c+d-w)^2}{R_R^2}\right] r\,dr\,d\theta$$

$$P_{\mathrm{III}} = 2\int_0^{\cos^{-1}[(d-u)/R_R]} \int_{(d-u)/\cos\theta}^{R_R} \left[1 - \left(\frac{r}{R_R}\right)^2\right] r\,dr\,d\theta$$

$$T = \frac{P_{\mathrm{I}} + P_{\mathrm{II}} + P_{\mathrm{III}}}{P_T}.$$

A.2 Case IV (Fig. 5) $d/R_T > 1 - K$ for $K < 1$.

$$P_{\mathrm{I}} = 4\int_0^{\pi/2} \int_0^{R_R} \left[1 - \left(\frac{r}{R_R}\right)^2\right] r\,dr\,d\theta - 2\int_0^{\cos^{-1}[(u-d)/R_R]} \int_0^{R_R} \left[1 - \left(\frac{r}{R_R}\right)^2\right] r\,dr\,d\theta - 2\int_0^{\cos^{-1}(p/c)} \int_{p/\cos\theta}^{c} \left[1 - \left(\frac{r}{R_R}\right)^2 - \frac{2r(c+w-d)\cos\theta}{R_R^2} - \frac{(c+w-d)^2}{R_R^2}\right] r\,dr\,d\theta$$

$$P_{II} = 2\int_0^{\cos^{-1}(p/c)} \int_{p/\cos\theta}^{c} \left[1 - \left(\frac{r}{R_T}\right)^2 - \frac{2r(c+w)\cos\theta}{R_T^2} - \frac{(c+w)^2}{R_T^2}\right] r dr d\theta$$

$$P_{III} = 2\int_0^{\cos^{-1}(u/R_T)} \int_{u/\cos\theta}^{R_T} \left[1 - \left(\frac{r}{R_T}\right)^2\right] r dr d\theta$$

$$T = \frac{P_I + P_{II} + P_{III}}{P_T}.$$

REFERENCES

1. A. H. Cherin and P. J. Rich, "A Multi-Groove Embossed Plastic Splice Connector for Joining Groups of Optical Fibers," Applied Optics, *14* (December 1975), pp. 3026–3030.
2. C. M. Miller, "Loose Tube Splices for Optical Fibers," B.S.T.J., *54* (September 1975), pp. 1215–1226.
3. C. M. Miller, "A Fiber Optic Cable Connector," B.S.T.J., *54* (November 1975), pp. 1547–1556.
4. F. L. Thiel, "Utilizing Optical Fibers in Communications Systems," International Conference on Communications, Conference Record, Vol. II, Session 32, June 16–18, 1975.
5. D. M. Henderson, "A Fiber Quick-Connect Coupler," unpublished work.
6. W. E. Pugh, "Geometric Considerations for Array Splices in Fiber Optic Cables," unpublished work.
7. C. M. Miller, "Loss vs Tranverse Offset for Parabolic Fiber Splices," unpublished work.
8. D. Gloge and E. A. J. Marcatili, "Multimode Theory of Graded-Core Fibers," B.S.T.J., *52* (November 1973), pp. 1563–1578.
9. T. C. Chu, unpublished data on transmission vs offset for parabolic fibers, June 23, 1975.
10. C. M. Miller, unpublished data on transmission vs offset for an array splice using parabolic fibers, October 1, 1974.
11. J. S. Cook, P. Balaban, and T. C. Chu, "Axial Displacement Loss in Fiberguide Connectors," unpublished work.
12. D. Marcuse, "Excitation of Parabolic-Index Fibers with Incoherent Sources," B.S.T.J., *54* (November 1975), pp. 1507–1530.
13. D. Gloge, "Offset and Tilt Loss in Optical Fiber Joints," B.S.T.J., this issue.